A SIMS and classical dynamics study of the chemisorption of CO on Ni{7 9 11}

K. E. Foley,[a] N. Winograd, and B. J. Garrison[b]
Department of Chemistry, The Pennsylvania State University, University Park, Pennsylvania 16802

D. E. Harrison, Jr.
Department of Physics and Chemistry, Naval Postgraduate School, Monterey, California 93940

(Received 19 September 1983; accepted 7 December 1983)

The dependence of secondary ion intensities on azimuthal angle of incidence of the primary ion beam in SIMS experiments on a stepped Ni{7 9 11} surface with adsorbed CO has been examined in detail. The surface was examined after various exposures to CO and at temperatures of 231 and 300 K. The angular anisotropies for the Ni^+, Ni_2^+, Ni_3^+, Ni_2CO^+, and especially the $NiCO^+$ species were found to be quite sensitive to surface structure changes suggested using other surface science techniques. Ion yield ratios as a function of exposure of CO to the surface, however, were found to be nearly insensitive to these structural changes. Of particular significance was the presence of a sharp feature in the $NiCO^+$ ion yield at an Ar^+ ion angle of incidence of $\phi = 110°$ with the crystal temperature at 231 K and after a CO exposure adequate to populate the step edge sites. At higher exposures or temperatures, this feature was washed out when presumably mostly terrace sites are occupied. Using these ion yield versus azimuthal angle curves, it is also apparent that the saturation coverage structures at 231 and 300 K are different. By introducing 10^{-7} Torr of CO into the chamber at 300 K the ion yield curves are identical to those for the saturation coverage at 231 K, indicating similar surface structures. Classical dynamics calculations aimed at modeling the structure corresponding to a CO exposure of 0.6 L at 231 K support the idea that the CO molecules reside in twofold bridge sites along the bottom of the step edge.

I. INTRODUCTION

The cluster formation and particle ejection process in secondary ion mass spectrometry (SIMS) has been shown to be related to the original arrangement of atoms or molecules on a single crystal surface.[1] For clean metals and clean metals covered with simple adsorbates, structural effects are strongly observable in measured azimuthal angle distributions of the ejected species. The reason for this effect is that the desorbing particles are directed in space by channels in the surface layer. Adsorbates may block or enhance the influence of these channels, an effect which is seen experimentally. Vertical channels created by larger organic molecules adsorbed perpendicular to the surface have recently been shown to be important in controlling the polar angle distribution of ejected molecular ions.[2] In all the above cases, classical dynamics calculations of the ion impact event have been useful in extracting mechanistic interpretations and in providing semiquantitative fits to the experimentally measured angular distributions.

Since both polar and azimuthal angle distributions are sensitive to subtle differences between surface structures, it is of interest to examine the role of larger irregularities such as surface steps on the measured quantities. For example, the orientation of the primary ion beam in the SIMS experiment can be fixed at different azimuthal angles with respect to the step edge. If the ejection process is structure sensitive, then changes in yields and cluster formation probabilities should be observed as the ion bombards "up" or "down" the steps. In addition, the desorption of chemisorbed molecules should be influenced by their proximity to the step edge.

Carbon monoxide chemisorption on Ni{7 9 11} represents a uniquely favorable case with which to check these concepts since comparable studies have been performed on Ni{001}[3] and Ni{111},[4] and since a number of other experimental methods have been applied to this system. Using the more descriptive nomenclature of Lang, Joyner, and Somorjai,[5] Ni{7 9 11} may also be identified as Ni(S)-[5{111}×{$\bar{1}$10}]. In this nomenclature Ni(S) indicates that this is a stepped nickel surface. The ordered step array is completely described by the width and orientation of the terraces and the height and orientation of the steps. Ni{7 9 11} has terraces of {111} orientation five atomic rows in width and steps of {$\bar{1}$10} orientation one atomic layer high as indicated by nomenclature [5{111}×{$\bar{1}$10}]. A hard sphere model of this surface is shown in Fig. 1(a). Erley, Wagner, Ibach, and Lehwald have investigated the chemisorption of carbon monoxide on Ni{7 9 11} using low energy electron diffraction (LEED), thermal desorption, auger electron spectroscopy (AES), and electron energy loss spectroscopy (EELS).[6,7] They conclude that the step edges lower the activation energy for CO decomposition. Work function measurements have shown that electrostatic dipole moments are associated with step edges.[8] The dipole is oriented such that the upper edge atom has a net positive charge and the lower terrace region has a net negative charge. Therefore, the CO molecules which adsorb on the lower terrace adjacent to the step edge acquire more negative charge into the antibonding π^* orbital[7] weakening the C–O bond. The electron energy loss studies were peformed mainly at 150 K and concentrated on the CO bonding geometries seen at low

[a] Present address: American Cyanamid Co., P. O. Box 60, 1937 W. Main St., Stamford, CT 06904.
[b] Alfred P. Sloan Research Fellow.

 0021-9606/84/105254-08$02.10 © 1984 American Institute of Physics

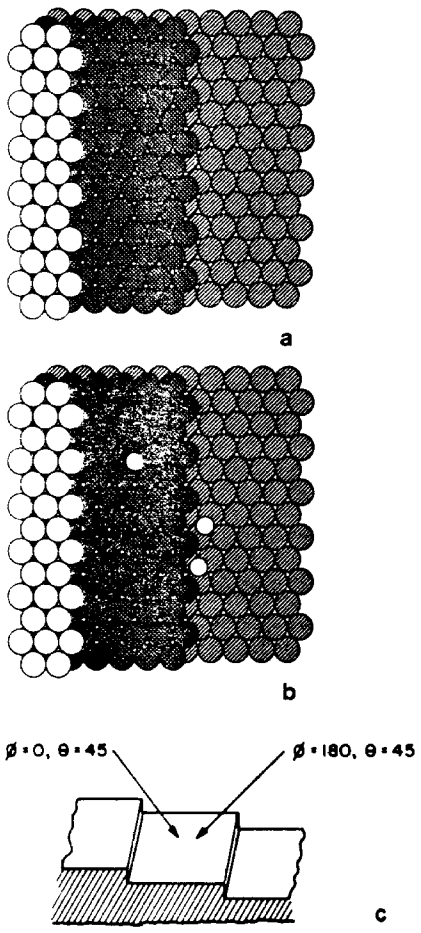

FIG. 1. Ni(7 9 11) surface. (a) Hard sphere model of the Ni{7 9 11} surface. (b) Hard sphere model of the Ni{7 9 11} surface showing three possible CO bonding sites. See the text for an explanation. (c) Definition of the polar (θ) and azimuthal (ϕ) angles of incidence of the primary ion beam relative to the Ni{7 9 11} surface.

exposures. These investigators[6,7] suggested that initial adsorption occurs in threefold and twofold bridge sites along the step edge as shown in Fig. 1(b). Beyond this point the CO molecules begin to occupy terrace sites, mainly the threefold bridge sites on the terrace [Fig. 1(b)]. Thus, the low temperature adsorption of CO on Ni{7 9 11} presents a realm of interesting structural phases which should be sensitive to the azimuthal angle of incidence of the primary ion beam. Room temperature adsorption of CO on Ni{7 9 11} has not been as well characterized, but it appears that the higher temperatures cause occupation of atop sites at the expense of the bridge step sites.[7] There is some evidence that the atop sites close to the step edge are occupied first.

In this study we examine the effect of changing the angle of incidence in SIMS experiments on the yields of ions ejected from a CO covered Ni{7 9 11} surface. The ion yields are measured as a function of CO exposure and at two surface temperatures 231 and 300 K. For virtually all the ions detected, both atomic and cluster species, bombardment down the step [$\phi = 0°$ azimuth of Figure 1(c)] causes fewer particles to be ejected than bombardment up the step ($\phi = 180°$ azimuth) where the ion can effectively peel off the step atoms. Surprisingly, however, the most intense yields occur at about $\phi = 60°$ or 120° azimuths which correspond to bombardment along the close packed rows of the {111} terrace. The ion yield vs azimuthal angle of incidence curves are dependent on the coverage of CO as well as on the surface temperature indicating that the ejection process is sensitive to atomic structure changes.

We also present a classical dynamics study aimed toward understanding the mechanisms of cluster formation on this system. Reasonable agreement with the experimental $NiCO^+$ ion yields is obtained if the CO molecules are placed in the proposed twofold bridge sites. The results from calculations with the carbon monoxide molecules in other adsorption sites do not agree as well with the experimental results. There is however only qualitative agreement between theory and experiment for the Ni^+ and Ni_2^+ ion yields.

The remainder of this paper is organized as follows: Section II gives the experimental details and Sec. III the calculational details. The results from the experiments and calculations are given in Secs. IV and V, respectively. The conclusions are presented in the final section.

II. EXPERIMENTAL

The SIMS experiments were performed on an instrument described previously[4] which is schematically shown in Fig. 2. The sample was mounted such that the polar angle of incidence θ of the 1 keV Ar^+ primary ion was fixed at 45°, but the azimuthal angle of incidence ϕ was continuously variable from 0° to 180°. These angles are defined relative to the structure of the surface shown in Fig. 1(c). The sample was cut from an MRC Ni{111} single crystal 9 mm in diameter. The crystal was oriented by Laue diffraction to expose the {111} face and a vicinal surface with an inclination of 10.3° was cut in the $\langle 1\bar{1}0 \rangle$ direction. The surface of the disc was mechanically polished, hot acid etched, and oriented by Laue diffraction to an accuracy of better than 1°. The crystal was then spot welded to the sample holder. The angular orientation was aligned with the manipulator markings by eye and is, therefore, only accurate to $\pm$ 10°. The crystal cleaning procedure consists of cycles of Ar^+ ion bombardment followed by annealing to 1200 K. Trace carbon impurities

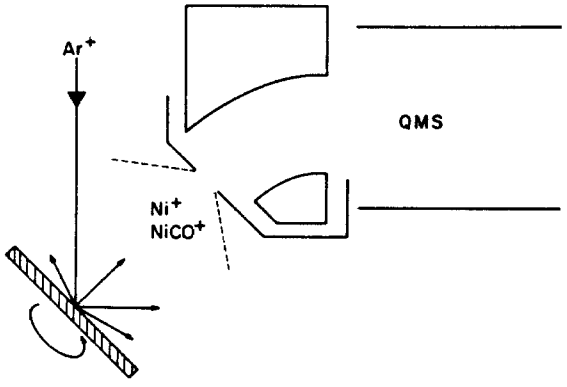

FIG. 2. Schematic diagram of the sample-detector configuration. The dotted lines indicate the approximate angle of acceptance of the quadrupole mass spectrometer (QMS).

were removed by heating to 900 K in 5×10^{-8} Torr O_2, sputtering, and then heating to 900 K in 5×10^{-8} Torr H_2. Cleaning was continued until the Ni^+ yield was extremely low (~25 cps) and the impurity K^+ was barely discernible above baseline. Bombardment of the crystal at an azimuthal angle of 90° gave much more efficient sputter cleaning than bombardment at angles of 0° or 180°. Sulfur was best removed by ion bombardment with a surface temperature of 500 K rather than at room temperature. The crystal could be resistively heated to 1200 K and cooled by liquid nitrogen to 230 K. The cooling was less efficient here than in the Ni{111} study because the azimuthal rotation required that the crystal be connected to a larger support which acted as a heat sink. The CO used in these experiments was 99.99% research grade purity from Matheson Gas Products.

III. DESCRIPTION OF THE CALCULATION

The basic scheme for computing the dynamics of the bombarding ion, the metal substrate, and the adsorbates has been described in detail elsewhere.[9–18] One step of the Ni{7 9 11} surface used in the calculations is shown in Fig. 3. For this model crystallite the Ar^+ ion must representatively sample an irreducible symmetry zone which extends over the whole width of a step terrace. However, if the Ar^+ ion strikes the crystal near the edge of the microcrystallite, the resulting trajectories are influenced by edge effects. To avoid this problem the calculation is performed by keeping the impact zone in the center of the crystallite and moving the step edge position so that the entire impact zone of Fig. 3 is sampled. This scheme is graphically displayed in Fig. 4. In each frame the central rectangular region represents the impact zone. The calculation of Ar^+ ion collisions within the impact zone for each of the five positions of the step edge, described as the 2*X*, 3*X*, 4*X*, 5*X*, and 6*X* positions, is equivalent to the calculations of the true Ni{7 9 11} surface without the computational difficulty of edge effects. At each position of the step edge, 104 impact points are run, summing to a total of 520 points for the complete Ni{7 9 11} surface. The results from any one position of the step edge are, of course, physically unrealistic. Only the sum of the results from all five step positions are comparable to the experimental results. The 1*X* and 7*X* positions are omitted since they represent a physically inaccurate Ni{7 9 11} surface in which the terraces are six, instead of five, atomic rows wide.

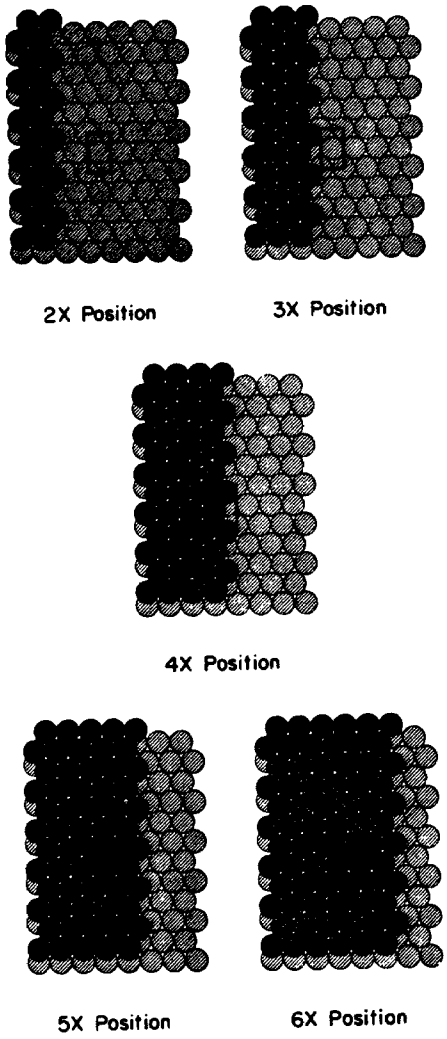

FIG. 4. The five different microcrystallites used in these calculations. The sum of these surfaces is equivalent to the Ni{7 9 11} surface shown in Fig. 3. The outlined regions are the impact zones.

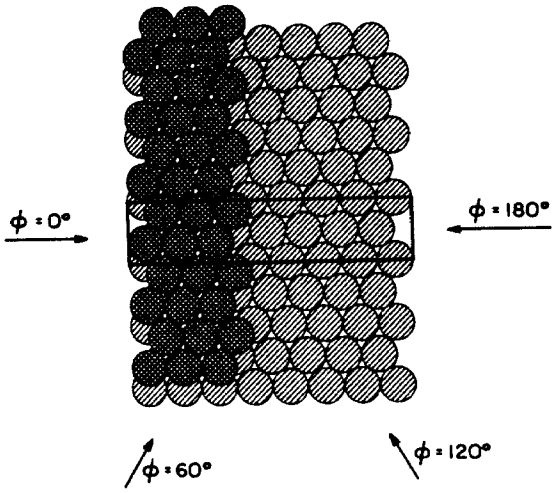

FIG. 3. A representation of the Ni{7 9 11} surface. The outlined rectangle represents the irreducible symmetry zone for this surface. The circles represent Ni atoms. The azimuthal angles of incidence are indicated.

Based on previous EELS studies,[6,7] the CO molecules are placed in either the twofold or threefold bridge sites along the step edge as shown in Fig. 5. A configuration where the CO molecules are placed in twofold bridge sites on a flat Ni{111} surface was also examined to determine the effect of the step edge on the CO ejection process. The binding energies and Ni–CO distances are estimated from available data for CO adsorbed on flat Ni surfaces. For CO adsorption on Ni{111}, the binding energy in the coverage regime of interest is 1.15 eV.[19,20] Crystal structure data has shown that a typical Ni–C distance for bridge bonds in metal–carbonyl complexes is 1.82 Å.[21] This value is used for the Ni–C distance in the calculations for two- and threefold bridge bonded CO. The bulk potential parameters given in

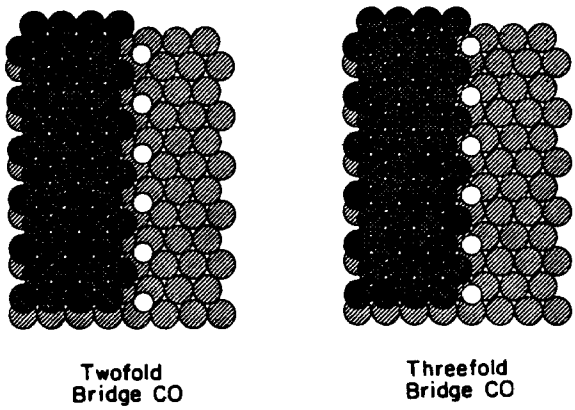

FIG. 5. Placements of the CO molecules. The shaded circles represent Ni atoms and the open circles are CO molecules.

Table I have been adjusted so that a Ni–C distance of 1.82 Å yields a binding energy of 1.15 eV between the CO molecule and the Ni{7 9 11} surface.

Three different potentials were employed to represent the $Ar^+ - Ni$, $-C$ and $-O$ interactions. The first is a Born–Mayer or exponential repulsion which has been used extensively in previous calculations.[9] The second is a Moliere interaction with a 1.0 scaling factor for the screening length.[3,22] The final potential is also of the Moliere form but with a scaling factor of 0.75. This latter interaction is closer to the R potential that has been found to work well for the interaction of Ar^+ ions bombarding copper sufaces.[17] For an initial kinetic energy of the Ar^+ ion of 1000 eV the Born–Mayer potential corresponds to the largest atom sizes and the Moliere with a scaling factor of 0.75 to the smallest. The Ni–Ni interaction is given in Ref. 9.

In an effort to reproduce the experimental data we have investigated the effect of both the CO adsorption site and the Ar^+ ion interaction potentials on the ejection yields as a function of the azimuthal angle of incidence of the primary ion. Similar calculations were also performed for the clean surface. In all cases the Ar^+ ion has 1000 eV of kinetic energy and is oriented at an angle of 45° with respect to the terrace normal. Note that to examine the effect of an adsorption site or potential yields that calculations for at least four to five azimuthal angles must be completed. Although not all the results will be presented in Sec. VI, a total of 62 different sets of calculations, each consisting of 520 Ar^+ ion impacts, have been performed. The total computational effort on a Floating Point System 120B array processor was approximately four months.

TABLE I. Potential parameters.

	D_e(eV)	β(Å^{-1})	R_e(Å)
Ni–O[a]	0.04	2.15	2.753
	0.04	2.15	2.666
Ni–C[a]	0.3374	2.59	1.82
	0.2533	2.59	1.82

[a] The top set of values applies to CO in a twofold bridged site and the bottom set to CO in a threefold bridged site.

IV. EXPERIMENTAL RESULTS AND DISCUSSION

The positive ion SIMS spectrum from the Ni{7 9 11} surface saturated with CO at room temperature is characterized by a series of molecular cluster ions including $NiCO^+$, Ni_2^+, and Ni_2CO^+. The form of the spectrum is virtually identical to that reported for Ni{100} and Ni{111},[3,4] illustrating that the presence of these peaks does not reflect differences in surface structure. Of more interest, however, is the behavior of the $Ni_2CO^+/NiCO^+ \times Ni^+/Ni_2^+$ ratio as a function of CO exposure. This ratio product has been proposed to be sensitive to the relative amount of CO in bridge and atop bonding geometries. In Fig. 6(a), we show the variations of this ratio with CO exposure for Ni{7 9 11} at 231 and 300 K while bombarding along $\phi = 180°$. The results are almost indistinguishable from those found on Ni{111} indicating that this data representation is insensitive to the presence of the atomic step. Other ion yield ratios have also been examined for Ni{7 9 11} and in each case, the results are nearly the same at 300 and at 231 K and are similar to those reported for Ni{111}. None of these ion yield ratios exhibit a simple correlation to the CO bonding geometry changes which have been proposed to occur using other surface techniques. The value of the azimuthal angle of incidence of the primary ion beam (with $\theta = 45°$) slightly influences the ion yield ratio curves. At $\phi = 110°$, particularly at 231 K as shown in Fig. 6(b), the $Ni_2CO^+/NiCO^+ \times Ni^+/Ni_2^+$ ratio product exhibits a definite minimum at 0.6 L exposure. This exposure is nearly the same exposure where EELS measurements suggest that all the bridge sites next to the step edge are occupied.

The secondary ion intensities of the molecular cluster ions turn out to be very sensitive both to ϕ of the primary

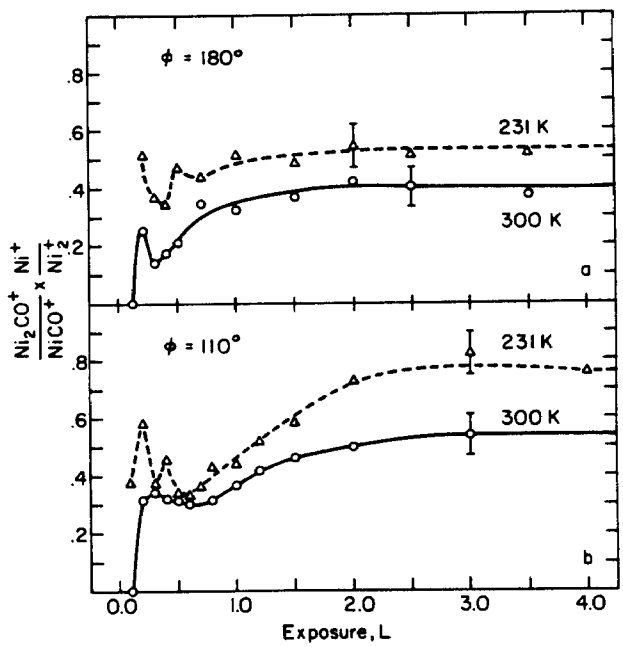

FIG. 6. Dependence of the ratio product $Ni_2CO^+/NiCO^+ \times Ni^+/Ni_2^+$ on CO exposure for Ni{7 9 11} at 300 K(—) and 231 K(---) with the 1000 eV Ar^+ bombarding at (a) $\theta = 45°$, $\phi = 180°$ and (b) $\theta = 45°$, $\phi = 110°$. The ratio values are not corrected for isotope distributions.

Ar^+ ion and to the surface structure itself. Before actually performing experiments to test this concept, we had expected to find marked differences between the yields obtained due to bombardment at $\phi = 0°$ and at $\phi = 180°$, with monotonic variation at intermediate angles. The experimental results for the Ni^+, Ni_2^+, and Ni_3^+ ion signals as a function at the azimuthal angle of incidence of the primary ion from clean Ni{7 9 11} are shown in Fig. 7. As seen in this and later figures, the ion intensities are usually higher at $\phi = 180°$ than at $\phi = 0°$ since at $\phi = 180°$, the Ar^+ ion effectively penetrates under the step edge, shearing away many surface atoms. The most interesting structure in these curves, however, appears at azimuthal angles of incidence between 0° and 180°. From the clean surface the Ni^+, Ni_2^+, and Ni_3^+ ion intensities all exhibit broad peaks for azimuthal angles of incidence between 110° and 140°. The Ni_2^+ and Ni_3^+ ion signals also show broad, smaller peaks between 60° and 90°. Since the ion yields from the clean surface are very low, these data are rather noisy, but the broad peaks are definitely above the noise level. The presence of these peaks can only be explained by assuming that they arise from ejection and cluster formation mechanisms which are favored at specific angles of incidence of the primary ion beam.

These azimuthal plots exhibit even more striking features as the Ni{7 9 11} surface is exposed to varying amounts of CO at 231 K, as illustrated in Fig. 8(a). The cluster ion yields are again higher at $\phi = 180°$ than at $\phi = 0°$, with the most significant variations occurring at intermediate angles. At 0.2 L exposure, the $NiCO^+$ ion signal shows a broad peak which appears at $\phi = 115°$. This peak shifts slightly to 105° and sharpens somewhat at an exposure of 0.4 L. By 0.6 L exposure the peak has become very intense and is only 10° wide, centered at $\phi = 110°$. As the CO coverage increases this peak becomes very broad. At the saturation exposure of 2.8 L the $NiCO^+$ ion intensity displays a broad maximum between $\phi = 40°$ and $\phi = 160°$. An exposure of 0.6 L corresponds almost exactly to the exposure at which the EELS results indicated that all the CO molecules are bound to adsorption sites near the step edge and that all the edge sites are occupied.[6,7] Apparently, the specific bonding site of the CO next to the step edge is responsible for the sharp peak in the $NiCO^+$ ion signal at $\phi = 110°$. At saturation, the peak loses this definition completely presumably since the CO molecules occupy several sites.

At CO exposures performed at room temperature the azimuthal plots do not exhibit such sharp features, as illustrated in Fig. 8(b). At exposures below 0.6 L, the $NiCO^+$ ion

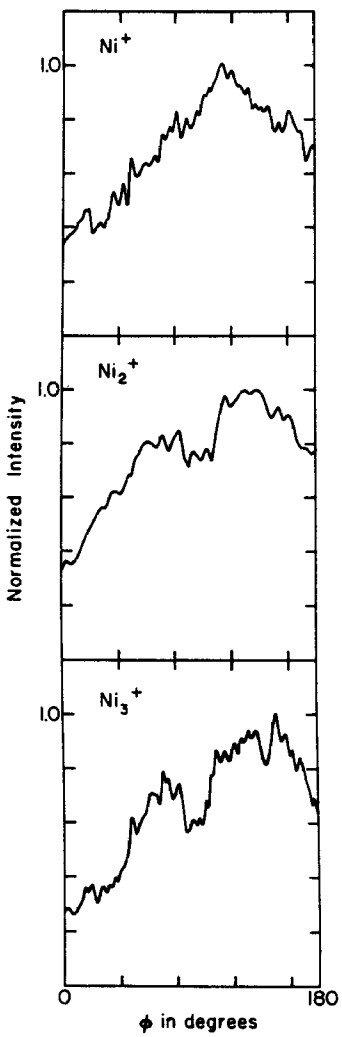

FIG. 7. Normalized Ni^+, Ni_2^+ and Ni_3^+ ion intensities from clean Ni{7 9 11} as a function of azimuthal angle of incidence with $\theta = 45°$ and a 1000 eV Ar^+ ion beam.

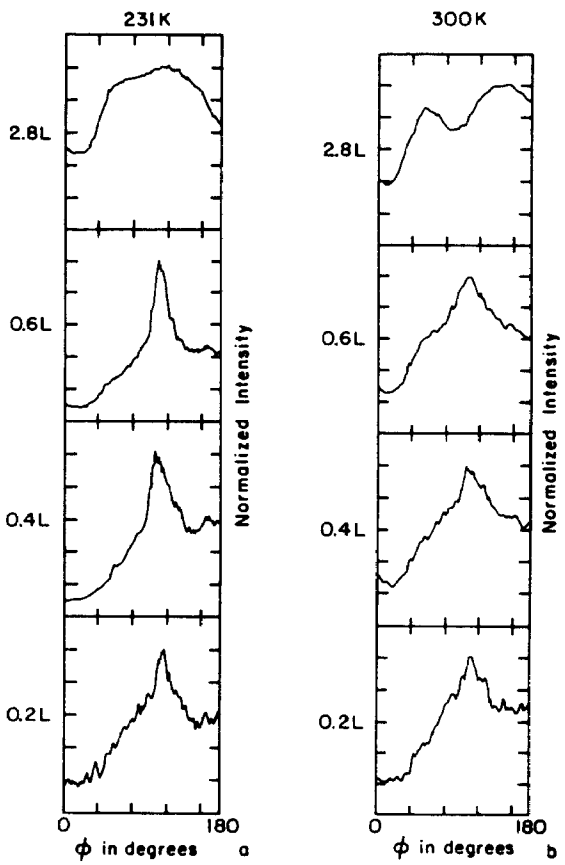

FIG. 8. Normalized $NiCO^+$ ion intensity versus azimuthal angle ϕ and as a function of CO exposure.

signal peaks at $\phi = 110°$, but the peak never becomes as sharp as during adsorption at 231 K. At saturation exposures, the peak in the $NiCO^+$ ion signal at $\phi = 110°$ has decreased and two broad peaks have appeared which are centered at $\phi = 50°$ and $\phi = 150°$. Note also that the shapes of the azimuthal plots are quite different for adsorption at 231 and at 300 K as indicated by comparing Figs. 8(a) and 8(b). It is reasonable to conclude that these changes are induced by differences in the CO bonding geometry, especially since the EELS results show that CO adsorbs on Ni{7 9 11} with less bonding specificity at room temperature than at 150 K.[6,7]

Although the variations in the $NiCO^+$ ion intensity with azimuthal angle of incidence are particularly unusual, there are also strong variations in the intensities of the other detectable ions. The magnitudes of the Ni^+, Ni_2^+, Ni_2CO^+, and Ni_3^+ ion signals as a function of azimuthal angle of incidence for CO adsorption at 231 K are shown in Fig. 9. At 0.2 L exposure the ion intensity curves are very similar to those from the clean surface. The Ni_2CO^+ ion signal exhibits very broad peaks at 80° and 120°, unlike the $NiCO^+$ signal. Even at 0.6 L exposure the Ni^+, Ni_2^+, and Ni_3^+ ion intensity curves are similar to those from the clean surface. At 0.6 L the Ni_2CO^+ signal displays a broad, poorly defined peak centered at an azimuthal angle of ~ 100°. An examination of these curves and their subtle changes with exposure indicates that the $NiCO^+$ ion intensity curve reflects most strongly the structural changes. At saturation the Ni^+, Ni_2^+, Ni_2CO^+, and Ni_3^+ intensity vs azimuthal angle of incidence curves do show significant differences from the 0.2 L exposure curves indicating some sensitivity to the changes in the CO overlayer. At this time, however, it is difficult to determine the actual structure of the overlayer by interpreting these curves or even to speculate as to why they have the shapes that they do.

It is apparent that the ion intensity vs azimuthal angle

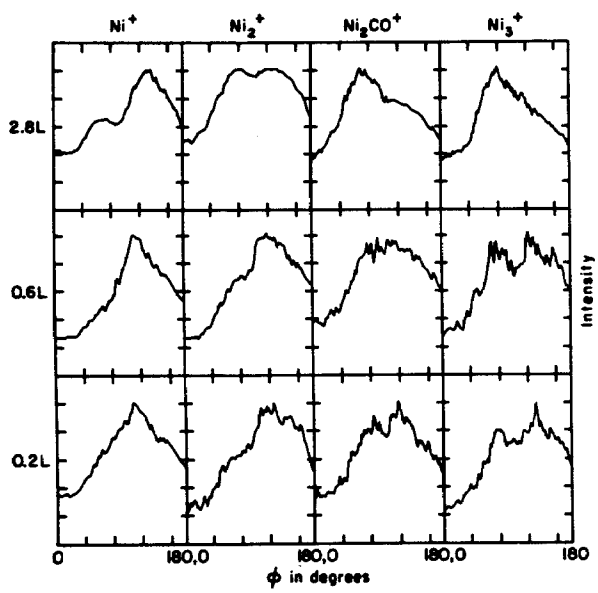

FIG. 9. Normalized Ni^+, Ni_2^+, Ni_2CO^+ and Ni_3^+ ion intensities from several CO exposures of Ni{7 9 11} at 231 K as a function of azimuthal angle of incidence.

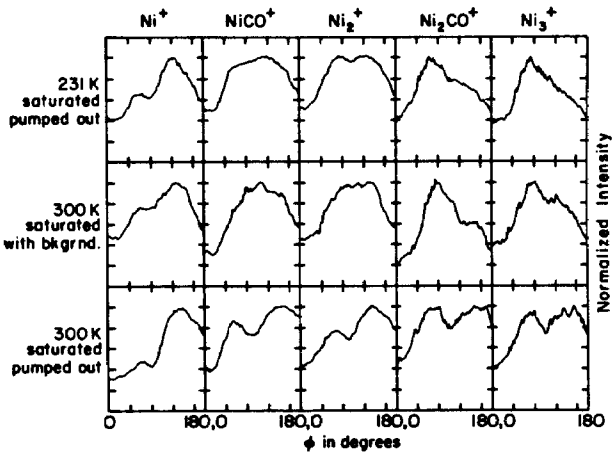

FIG. 10. Normalized Ni^+, Ni_2^+, Ni_2CO^+, and Ni_3^+ ion intensities from the following CO overlayers on Ni{7 9 11} as a function of azimuthal angle of incidence: CO saturated at 231 K, data taken at ambient presssure; CO saturated at 300 K, data taken at 1×10^{-7} Torr background pressure; CO saturated at 300 K, data taken at ambient pressure.

of incidence curves produce a myriad of patterns which are dependent upon conditions of the CO exposure to Ni{7 9 11}. Although it is not always possible to fully interpret the curves, the results may provide important "fingerprint" information. This point is illustrated in Fig. 10 where different ion signal variations are displayed for three different CO overlayer preparations on Ni{7 9 11}. In the first case, the sample was exposed at 231 K to enough CO to saturate the edge and terrace adsorption sites. Next, the same procedure was performed at 300 K to yield the curves shown in the bottom set of panels in Fig. 10. Although the variations in the Ni^+ ion signals are very similar, the other cluster ion yields exhibit large differences, strongly implying that there has been a marked change in the preferred CO bonding sites. In the middle example shown in Fig. 10, the spectra were recorded at 300 K with the crystal exposed to a 1×10^{-7} Torr CO background pressure. This condition resulted in another set of curves which are almost identical to the curves obtained at 231 K with no background pressure of CO. Apparently, then, it is possible in this case to obtain similar surface structures by either lowering the crystal temperature or by raising the overpressure of CO.

V. COMPARISON OF EXPERIMENTAL RESULTS TO CLASSICAL DYNAMICS CALCULATIONS

By comparison to classical dynamics calculations, it is possible to obtain a semiquantitative feeling for the meaning of the experimental plots shown in Figs. 7–9. Using the procedure outlined in Sec. III, we have modeled the Ar^+ ion bombardment of the Ni{7 9 11} surface under the following conditions: (i) clean (i.e., Fig. 3); (ii) with CO adsorbed in twofold sites along the step edge [Fig. 5(a)]; (iii) with CO adsorbed in threefold sites along the step edge [Fig. 5(b)]; and (iv) with a line of CO molecules adsorbed in twofold sites on a Ni{111} surface like that shown in Fig. 5 but with the atomic step missing. It is presumed that a comparison of case (ii) to case (iv) should yield information concerning the influence of the step itself on the CO ejection pathways. The strongest feature in the experimental plots is the sharp peak exhibited

by the $NiCO^+$ ion after exposure of Ni{7 9 11} to 0.6 L of CO at 231 K. We have therefore focused our attention on the calculated NiCO yield as a function of the azimuthal angle of the incident ion. The Ni and Ni_2 yields for both the clean surface and the CO covered surface are also discussed briefly.

A number of correction factors must be applied to the calculated results before they can be compared directly with the experiment. First, the energy bandpass of the prefilter on the mass spectrometer is fairly wide, but is not known accurately. From measured secondary ion energy distributions, we estimate that ions between 0 and 30 eV are being collected and have used this cutoff to select the number of calculated ejected species. This correction induces small changes in the calculated Ni distributions, but does not influence the yields of Ni_2 or NiCO species since they tend to have low kinetic energies. The second correction involves the acceptance angle of the energy prefilter. Since an extraction voltage was applied to the front lens element shown in Fig. 2, we assume that this acceptance angle is quite large. Our best estimate from geometrical considerations is that the polar angle resolution is $\pm$ 30° at normal emission. The calculated yields, as we shall demonstrate, are not very sensitive to the value selected for this parameter. Finally, a correction is necessary to account for the image force which will be exerted on the ejecting ion, but which is not included in the calculated trajectories of the neutrals. Previous studies of CO on Ni{100} have shown that good agreement between measured and calculated distributions are obtained when an image energy is subtracted from the perpendicular component of the kinetic energy of the ejecting species.[18] Since there is no way to calculate the magnitude of the image energy directly, we have used its value as a fitting parameter to maximize agreement between experiment and calculation as suggested previously.

The best fit to the experimental results arises from the calculations using a Moliere potential with a scaling factor of 1.0 and with the CO placed in a twofold bridge site. The polar angle resolution is $\pm$ 30° from the normal and the image energy correction is 2.4 eV. These results as well as those from using slightly different polar resolutions and image energies are shown in Fig. 11(a). Using these same parameters the predicted curves for other CO adsorption sites and Ar^+ interaction potentials are shown in Fig. 11(b). Attempts to fit the threefold bridge site case (iii) or the line of CO molecules on the step terrace, case (iv), to the experimental results were not as successful as attempts to fit the data shown in Fig. 11(a). It is interesting that CO adsorbed in a threefold bridge edge site did not contribute to the peak at $\phi = 110°$–120°. This observation is in disagreement with the EELS study where the presence of an anomalously low CO stretching frequency of 1520 cm^{-1} was assigned to the presence of this species, in concentrations equal to that of the twofold bridge species. It is not yet clear as to whether this disagreement arises from a misinterpretation of the 1520 cm^{-1} peak or to a deficiency in the SIMS calculations, perhaps one related to the neglect of the ionization phenomena.

The molecular dynamics scheme allows the evolution of the collision cascade to be monitored on an atomic level so that the mechanisms that give rise to particle ejection may be

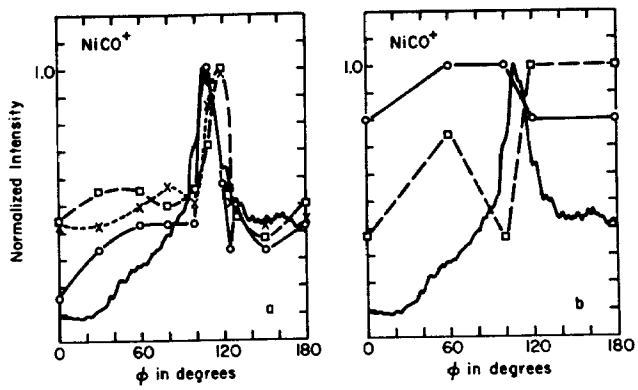

FIG. 11. Calculated NiCO yields versus azimuthal angle ϕ. In both frames the solid lines are the experimental results. (a) The CO is in a twofold bridge site and the Moliere potential with a scaling factor of 1.0 is used. O—polar angle resolution is $\pm$ 30° and the image correction energy is 2.4 eV; ×—polar angle resolution is $\pm$ 30° and the image correction energy is 1.8 eV; □—polar angle resolution is $\pm$ 40° and the image correction energy is 2.4 eV. (b) The polar angle resolution is $\pm$ 30° and the image correction energy is 2.4 eV. □—CO in a threefold bridge site using the Moliere potential with a scaling factor of 1.0; O—CO in a twofold bridge site on a flat surface using the Moliere potential with a scaling factor of 1.0.

elucidated in detail. We have attempted to utilize this aspect of the theory to determine why the sharp feature for the NiCO cluster should appear at $\phi = 110°$–120°. In general, these species are not composed of Ni atoms and CO molecules that were originally bonded together on the surface. The recombination mechanism of cluster formation[1,9] clearly dominates in producing NiCO molecules. We could not identify, however, a specific, structure sensitive ejection mechanism that yields the peak at $\phi = 110°$–120°. The only correlation we could find among the NiCO molecules is that approximately half of them contain the fifth CO molecule up from the bottom of Fig. 5(a). These clusters also arise mainly from bombardment with the step edge in the $2X$ and $3X$ positions.

Assuming that using the Moliere potential with CO placed in the twofold bridge site is appropriate we employed the same calculations to examine the Ni and Ni_2 yields (Fig. 12). Here the polar resolution of $\pm$ 30° is maintained but the image energy has been readjusted to maximize agreement with experiment. This agreement for both the clean and CO covered surfaces is not outstanding although there is some hint of a peak at $\phi = 120°$. The main failing is that the intensity of $\phi = 0°$ is too large in all cases. This deficiency is present in virtually all the calculation we performed on this stepped system.

There are many possible reasons why the structural features for the Ni and Ni_2 species are not well reproduced by the calculations. The ionization process is very sensitive to the local electronic environment near the ejection point. The step edge may either enhance or suppress the formation of ions that eject near it. The same interaction potentials have been employed for all atoms of the same type with no distinction made for position in the solid. For example, Ni atoms at the step edge are given the same pair potential as Ni atoms in the bulk. Until more is known about the mechanism of the

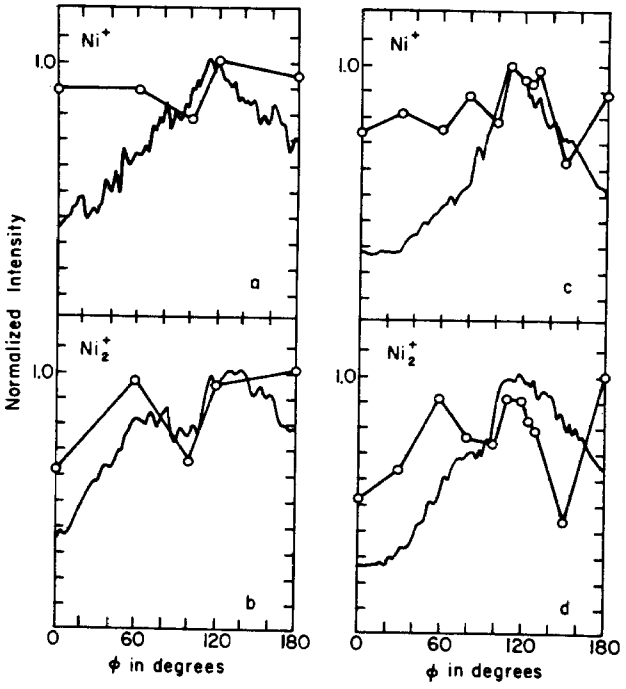

FIG. 12. Ni and Ni_2 yields vs azimuthal angle ϕ. The solid lines are the experimental results and the points are from the calculation using the Moliere potential with a scaling factor of 1.0. In all cases the polar angle resolution is $\pm 30°$ and the energy bandpass is 0 to 30 eV. The image correction energy for the Ni species is 3.6 eV and for the Ni_2 species is 2.4 eV. (a) Ni from the clean stepped surface. (b) Ni_2 from the clean stepped surface. (c) Ni from stepped surface with CO molecules in a twofold bridge site. (d) Ni_2 from the stepped surface with CO molecules in a twofold bridge site.

ionization process and the interaction potential describing step edges, it will be difficult to extract the reasons for differences between the calculated and experimental results.

VI. CONCLUSIONS

We have examined the dependence of ion intensity on azimuthal angle of incidence of the primary ion beam in SIMS experiments on a stepped Ni{7 9 11} surface with adsorbed CO. The Ni^+, Ni_2^+, Ni_3^+, Ni_2CO^+, and especially the $NiCO^+$ ion yields exhibit strong angular anisotropies. For example, the $NiCO^+$ yield is relatively small if the primary ion beam bombards down the step ($\phi = 0°$). The yield sharply peaks at $\phi = 110°$ and falls off to approximately one half the peak value for bombardment up the step ($\phi = 180°$). This behavior occurs only at 231 K and after CO exposures sufficient to populate the step edge adsorption sites. These azimuthal plots lose most of their structure when there is sufficient CO to populate the terrace sites. The ion yields can be used to "fingerprint" a particular surface structure. For example, the ion intensity curves taken at 231 and 300 K are quite different, but if at 300 K the chamber is filled to 10^{-7} Torr of background CO pressure the ion intensities are the same as at 231 K indicating that the surface structures in these two situations are similar. Classical dynamics calculations have been performed to attempt to understand the meaning of the anisotropies. Agreement with the NiCO intensity vs azimuthal angle is found if the CO molecules are situated in twofold bridge sites along the step edge. Only qualitative agreement of the Ni^+ and Ni_2^+ yields could be obtained.

ACKNOWLEDGMENTS

The financial support of the National Science Foundation, the Office of Naval Research, the Air Force Office of Scientific Research and the Petroleum Research Foundation administered by the American Chemical Society, is gratefully acknowledged. B. J. G. also thanks the Alfred P. Sloan Foundation for a Research Fellowship and the Camille and Henry Dreyfus Foundation for a grant for newly appointed faculty.

[1] B. J. Garrison and N. Winograd, Science **216**, 805 (1982); N. Winograd, Prog. Solid State Chem. **13**, 285 (1982) and references therein.
[2] D. W. Moon, R. J. Bleiler, E. J. Karwacki, and N. Winograd, J. Am. Chem. Soc. **105**, 2916 (1983).
[3] K. E. Foley and N. Winograd, Surf. Sci. **122**, 541 (1982).
[4] K. E. Foley and N. Winograd, Surf. Sci. **116**, 1 (1982).
[5] B. Lang, R. W. Joyner, and G. A. Somorjai, Surf. Sci. **30**, 440 (1972).
[6] W. Erley and H. Wagner, Surf. Sci. **74**, 333 (1978).
[7] W. Erley, H. Ibach, S. Lehwald, and H. Wagner, Surf. Sci. **83**, 585 (1979).
[8] K. Besoche, B. Krahl-Urban, and H. Wagner, Surf. Sci. **68**, 39 (1977).
[9] N. Winograd, B. J. Garrison, and D. E. Harrison, Jr., J. Chem. Phys. **73**, 3473 (1980).
[10] D. E. Harrison, Jr., W. L. Gay, and H. M. Effron, J. Math. Phys. **10**, 1179 (1969).
[11] D. E. Harrison, Jr., P. W. Kelly, B. J. Garrison, and N. Winograd, Surf. Sci. **76**, 311 (1978).
[12] B. J. Garrison, N. Winograd, and D. E. Harrison, Jr., J. Chem. Phys. **69**, 1440 (1978).
[13] N. Winograd, D. E. Harrison, Jr., and B. J. Garrison, Surf. Sci. **78**, 467 (1978).
[14] B. J. Garrison, N. Winograd, and D. E. Harrison, Jr., Phys. Rev. B **18**, 6000 (1978).
[15] B. J. Garrison, N. Winograd, and D. E. Harrison, Jr., Surf. Sci. **87**, 101 (1979).
[16] B. J. Garison, J. Am. Chem. Soc. **104**, 6211 (1982).
[17] D. E. Harrison, Jr., J. Appl. Phys. **52**, 1499 (1981).
[18] R. A. Gibbs, S. P. Holland, K. E. Foley, B. J. Garrison, and N. Winograd, Phys. Rev. B **24**, 6178 (1981); J. Chem. Phys. **76**, 684 (1982).
[19] K. Christmann, O. Schober, and G. Ertl, J. Chem. Phys. **60**, 4719 (1974).
[20] G. W. Rubloff, Surf. Sci. **89**, 566 (1979).
[21] R. J. Behm, K. Christmann, and G. Ertl, J. Chem. Phys. **73**, 2984 (1980).
[22] I. M. Torrens, *Interatomic Potentials* (Academic, New York, 1972).